A new method for the representation and evolution of three dimensional discontinuity surfaces in XFEM/GFEM

(Article begins on next page)

04 June 2023

A new method for the representation and evolution of three dimensional discontinuity surfaces in XFEM/GFEM

Giulio Ventura[1]
[1]*Department of Structural and Geotechnical Engineering, Politecnico di Torino, Italy*
E-mail: giulio.ventura@polito.it

SUMMARY. The ability of the extended and generalized finite element methods of modeling discontinuities independent of mesh alignment requires a suitable representation for the discontinuity surfaces. In the present paper a method for constructing level set functions based on vector data and geometric operations in three dimensions is presented. In contrast to classical level set methods, the proposed approach does not require the integration of differential evolution equations, resulting in a particularly simple structure and easy implementation.

1 INTRODUCTION

The inclusion of discontinuities or interfaces in the framework of the extended (XFEM) [1] or generalized (GFEM) [2] finite element methods is particularly straightforward, as arbitrary kind of discontinuities can be introduced by enriching the finite element space with customized functions whose analytical properties reflect the kind of discontinuity to be represented. These methods had a large diffusion in the last decade and software companies have started implementing these methods in commercial codes as their structure is particulary simple and their numerical efficiency is very high. In particular, the feature that discontinuity surfaces do not have to be aligned with finite element sides allows to skip remeshing for moving or evolving discontinuities.

One of the open research fields in the application of these methods is the efficient representation of three dimensional discontinuity surfaces. Several approaches have been presented, ranging from describing the surface by a 3D mesh of 2D elements to the use of level set functions [3, 4]. In particular, level set methods have their origin in the observation that no geometric representation of the surface is useful in XFEM/GFEM implementations, but the knowlwdege of the distance of Gauss or nodal points from the surface or its front. In this sense, the representation of the surface by meshes is a computational waste. On the other hand, level set methods store usually the distance from the surface at nodal points and level set differential evolution equations are used for updating level set data as the discontinuity surface evolves [5, 6, 7, 8]. These evolution equations are often quite complex to be implemented and some issues in freezing the data around the already formed surface parts have to be taken into account [9]. For the above reasons, the use of level set differential evolution equations is more convenient for moving interfaces, e.g. solidification problems [10], rather than some classes of mechanical problems like fracture, where once the discontinuity surface is formed it can expand but not move or vanish.

In the present paper a different and very efficient method is introduced. The method originates from the idea of "vector level sets" introduced in [11] and extends it to three dimensional problems. Given vector data on the evolution of the surface front (position and displacement of control points), distance data are computed at points and stored as nodal quantities by a purely geometric method, which is much simpler compared to classical level sets methods, requiring the integration of a set of differential evolution equations in a suitable domain around the discontinuity surface.

2 XFEM/GFEM APPROXIMATION AND LEVELSET FUNCTIONS

In order to introduce the need for level set functions data in XFEM/GFEM, it is useful to recall the displacement approximation adopted in these methods. Reference will be made to crack problems as this kind of interface, characterized by the formation and expansion of a discontinuity surface, is best suited to the vector level set method we will introduce in the next Section.

Consider a cracked body finite element model, Fig. 1. Let $\mathcal{S}$ be the set of all finite element nodes, $\mathcal{S}_C$ the set of element nodes around the crack front and $\mathcal{S}_H$ the set of nodes of elements completely cut by the crack. For crack problems two enrichments are considered: the Heaviside (step) function H for modeling displacement jump and a set Ψ^j of enrichment functions for representing the near tip (or front, in 3D) solution features. These enrichment functions can be expressed in terms of distance functions from the surface f and from the tip (or front) g that are, provided a proper scaling so that their gradient is unity, the level set functions of the crack surface and front, respectively. Under the above assumptions the XFEM displacement field for a crack is

$$\mathbf{u}\left(\mathbf{x}\right)=\sum_{\forall I}N_I\left(\mathbf{x}\right)\mathbf{u}_I+\sum_{J\in\mathcal{S}_H}N_J\left(\mathbf{x}\right)H\left(f(\mathbf{x})\right)\mathbf{q}_J^0+\sum_j\sum_{K\in\mathcal{S}_C}N_K\left(\mathbf{x}\right)\Psi^{(j)}\left(f(\mathbf{x}),g(\mathbf{x})\right)\mathbf{q}_K^{(j)} \quad (1)$$

where $\mathbf{u}_I$, $\mathbf{q}_J^0$, $\mathbf{q}_K^{(j)}$ are nodal and enrichment variables.
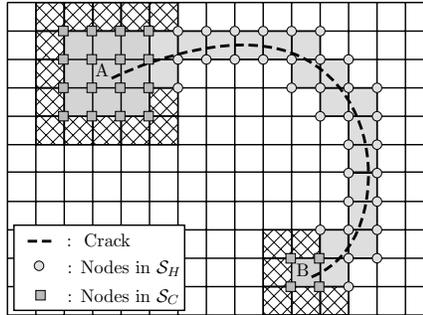

Figure 1: An arbitrary crack line (dashed line) in a structured mesh with step enriched (light gray) and tip enriched (gray) elements. Nodes in sets $\mathcal{S}_C$ and $\mathcal{S}_H$ are denoted by squares and circles, respectively. Cross hatched elements are partially enriched and require special treatment [12].

3 3D VECTOR LEVEL SET METHOD

In this section the vector level set functions and domains for the description of a 3D crack surface are introduced. The geometric update algorithm for the level sets as the crack surface evolves is presented as well. Note that the procedure described here is independent of the actual method chosen to solve the mechanical problem, e.g. finite elements, mesh free methods etc. and, as will be apparent in the following, it requires just a set of points where the vector level set functions are defined. These can be either the discretization nodes and/or any other selected set of points.

3.1 Crack surface modelling for vector level set data computations

The crack front at time t is assumed as described by an ordered sequence of line segments $\mathbf{t}_i$, Fig. 2(a). Let N_{cf}^t the number of nodal points $\mathbf{x}_i$ along the crack front. As will be apparent in the following, the sign convention for the level set functions is induced automatically by the orientation of the curvilinear abscissa along the crack front.
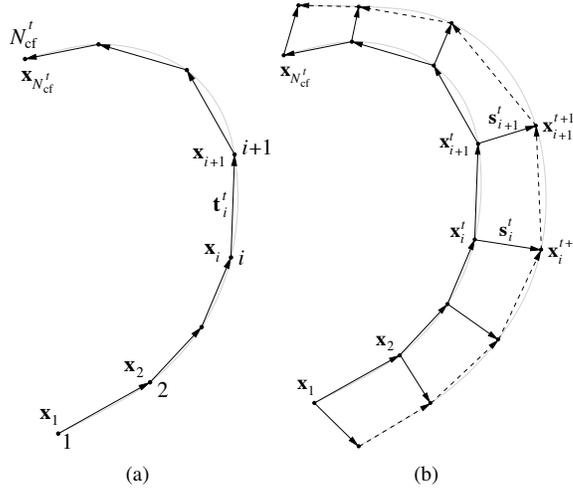

Figure 2: (a) Crack front description by an ordered sequence of line segments; (b) Crack front evolution by advance vectors at nodal points.

The crack front evolution is computed as crack advance vectors $\mathbf{s}_i^t$ at the N_{cf}^t nodal points so that, at time $t + 1$, the new crack front is defined by the same number of nodal points and line segments, see Fig. 2(b). The advance vectors $\mathbf{s}_i$ are in general non parallel nor coplanar.

The crack surface advance can be represented geometrically by a sequence of $N_{\mathrm{cf}}^t - 1$ four sided bilinear surfaces, each one having vertexes $\mathbf{x}_i^t$, $\mathbf{x}_{i+1}^t$, $\mathbf{x}_{i+1}^{t+1}$, $\mathbf{x}_i^{t+1}$, Fig. 2(b). These surface elements will be used to represent the crack surface advance and compute the level set functions. After the level set computation they will be no longer necessary to the crack surface representation. The crack surface advance represented as a collection of non-planar bilinear quadrilaterals will have slope discontinuities both between two adjacent elements of the crack front, and along the front between two subsequent front advance steps. These discontinuities will be called in the following *kink wedges*. Two families of kink wedges will be present, one running along the advance vectors and the other running along the crack front, see Fig. 3.

In computing the closest point projection of a generic point onto the crack surface advance two cases will then be possible. Either the closest point projection is an orthogonal projection on a crack surface element or it is a projection along a kink wedge.

In the next section the problem of the projection of a point on a single crack surface element will be addressed. Given a point and the crack front advance, the closest point projection will be determined by looping on the crack surface elements. This allows for both stating the existence of
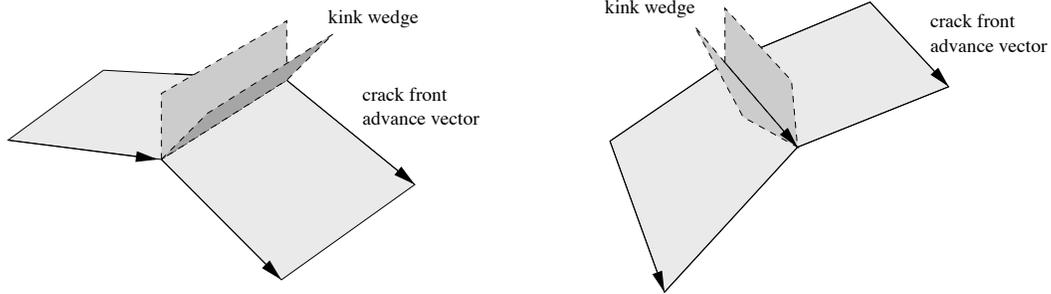
Figure 3: The concept of kink wedge: the nodes belonging to the space in between the two shaded planes have no orthogonal projection onto the crack surface elements. On the left the kink wedge runs along a crack front, on the right the kink wedge runs along the advance vectors.

an orthogonal projection on the element and for detecting points having projection along the kink wedges.

3.2 *Level set function f – Distance from the crack surface*

We assume that the level set function f at a point $\mathbf{P}$ can be expressed through a vector $\mathbf{f}$ and a Boolean H_f assuming the values ± 1 and yielding the sign of the distance, i.e. the side of the crack where the evaluation point $\mathbf{P}$ is located.

Figure 4 illustrates the definition of f and H_f in a bidimensional setting as well as the level set function g that will be introduced in the following.
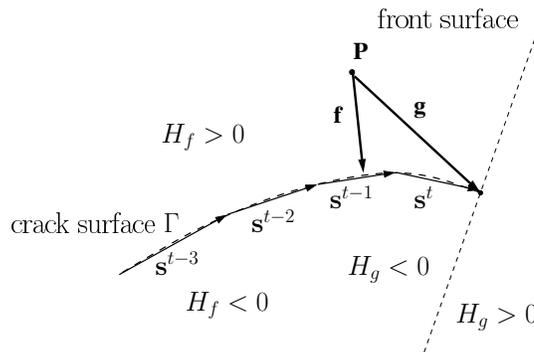

Figure 4: 2D illustration of the levelset functions f and g.

Given a generic point $\mathbf{P}$, at a time t, $\mathbf{f}(\mathbf{P}, t)$ is the vector $\mathbf{f} = \mathbf{P}' - \mathbf{P}$ where $\mathbf{P}'$ is the closest point projection of $\mathbf{P}$ onto Γ. The signed distance function $f(\mathbf{P}, t)$ can be computed through the

formula $f(\mathbf{P}, t) = \|\mathbf{f}(\mathbf{P}, t)\| \, H_f(\mathbf{P}, t)$. In the following sections the level set function and domain update are detailed.

3.2.1 Representation of surface elements and point projection.

The single crack surface element is defined by the position of its four corners in space. It can be therefore represented by the isoparametric concept applied to the non planar quadrilateral of vertexes $\mathbf{x}_i^t, \mathbf{x}_{i+1}^t, \mathbf{x}_{i+1}^{t+1}, \mathbf{x}_i^{t+1}$, Fig. 5. All the subsequent development can be readily extended to higher order isoparametric representations of the crack surface.
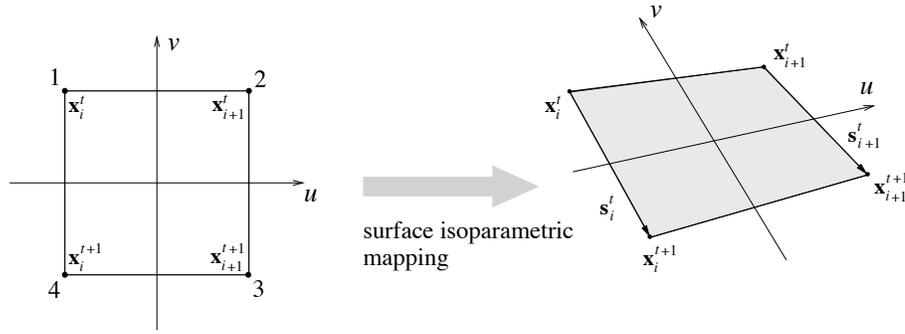

Figure 5: Linear isoparametric description of a crack surface element.

Let $g(u, v)$, $u, v \in [-1, 1]$ the standard shape functions for the element

$$g_1(u, v) = \frac{1}{4}(1 - u)(1 + v), \quad g_2(u, v) = \frac{1}{4}(1 + u)(1 + v) \tag{2}$$

$$g_3(u, v) = \frac{1}{4}(1 + u)(1 - v), \quad g_4(u, v) = \frac{1}{4}(1 - u)(1 - v) \tag{3}$$

The crack surface element is given by the following parametric equations $\phi(u, v), u, v \in [-1, 1]$, Fig. 5,

$$\begin{cases} \phi_x = g_1(u, v) \, x_i^t + g_2(u, v) \, x_{i+1}^t + g_3(u, v) \, x_{i+1}^{t+1} + g_4(u, v) \, x_i^{t+1} \\ \phi_y = g_1(u, v) \, y_i^t + g_2(u, v) \, y_{i+1}^t + g_3(u, v) \, y_{i+1}^{t+1} + g_4(u, v) \, y_i^{t+1} \\ \phi_z = g_1(u, v) \, z_i^t + g_2(u, v) \, z_{i+1}^t + g_3(u, v) \, z_{i+1}^{t+1} + g_4(u, v) \, z_i^{t+1} \end{cases} \tag{4}$$

The parametric surface $\phi(u, v)$, Eq. (4), allows for the definition of the normal to the surface element. In fact, by differential geometry, the cartesian equation of the tangent plane Π_0 to the surface $\phi(u, v)$ at (u_0, v_0) is given by the symbolic determinant

$$\det \begin{bmatrix} x - \phi_x(u_0, v_0) & y - \phi_y(u_0, v_0) & z - \phi_z(u_0, v_0) \\ \phi_{x,u}(u_0, v_0) & \phi_{y,u}(u_0, v_0) & \phi_{z,u}(u_0, v_0) \\ \phi_{x,v}(u_0, v_0) & \phi_{y,v}(u_0, v_0) & \phi_{z,v}(u_0, v_0) \end{bmatrix} = 0 \tag{5}$$

5

where $,u$ and $,v$ denote the partial derivatives w.r.t. the variables u and v, respectively. Consequently, denoting with $A(u_0, v_0)$, $B(u_0, v_0)$ and $C(u_0, v_0)$ the minors

$$A(u_0,v_0) = \begin{vmatrix} \phi_{y,u} & \phi_{z,u} \\ \phi_{y,v} & \phi_{z,v} \end{vmatrix}, \; B(u_0,v_0) = - \begin{vmatrix} \phi_{x,u} & \phi_{z,u} \\ \phi_{x,v} & \phi_{z,v} \end{vmatrix}, \; C(u_0,v_0) = \begin{vmatrix} \phi_{x,u} & \phi_{y,u} \\ \phi_{x,v} & \phi_{y,v} \end{vmatrix} \quad (6)$$

the vector of the normal to the parametric surface at (u_0, v_0) is given by $\mathbf{n}(u_0, v_0) = (A, B, C)$ and is such that the axes u, v and the positive direction of n form a right-handed cartesian coordinate system. The cartesian equation of the tangent plane to the parametric surface is

$$A(u_0,v_0)\,(x - \phi_x(u_0,v_0)) + B(u_0,v_0)\,(y - \phi_y(u_0,v_0)) + C(u_0,v_0)\,(z - \phi_z(u_0,v_0)) = 0 \quad (7)$$

Let now $\mathbf{P} \equiv (x_p, y_p, z_p)$ the position vector of a generic point in the cartesian space, and suppose an orthogonal projection $\mathbf{P}'$ onto a parametric surface element exists. The position vector of $\mathbf{P}$ can be expressed by the sum of its projection vector onto the surface plus the position vector of the projected point $\mathbf{P}'$, i.e. $\mathbf{P}$ is the sum of its projection, given parametrically by $\mathbf{P}'(u, v)$, and the normal vector at $\mathbf{P}'$ scaled by a factor λ to be determined

$$\mathbf{P} = \mathbf{P}'(u,v) + \lambda\,\mathbf{n}(u,v) \quad (8)$$

The above vector equation is equivalent to three scalar equations in the three unknowns u, v, λ. In the hypothesis the orthogonal projection exists, the solution to (8) in the variables u, v, λ is such that $u, v \in [-1, 1]$ and $d = \lambda \|\mathbf{n}(u, v)\|$ represents the signed distance of $\mathbf{P}$ to the parametric surface, the sign being induced by the sign of λ. On the contrary, when solving (8) u and/or $v \notin [-1, 1]$ is obtained. Then the projection is not onto the crack surface element but on the analytic continuation of its parametric representation $\phi(u, v)$. In this case the orthogonal projection in the interior the crack surface element does not exists, but a closest point projection on the kink wedges may be possible, see Fig. 6.

Once a point is determined to belong to a kink wedge its closest point projection is determined geometrically by point to segment distance. In all cases the scalar H_f is given by $H_f = \text{sign}(\lambda)$.

3.2.2 Vector level set f-domain definition and evolution

Let $\mathcal{F}^t$ be the set of nodes over which the function f is defined at time t. As the crack evolves, given the crack front and the advance vectors $\mathbf{s}_i^t$, the set of nodes where the signed distance is to be computed is given by all the nodes belonging to the elements intersected by the crack surface advance and will be named $\mathcal{F}_a^t$. For each node in the set $\mathcal{F}_a^t$, the projection onto the crack surface advance is computed by the method described in the previous section. Then $\mathcal{F}_a^t$ is divided into the sum of the following two disjoint sets:

$$\mathcal{F}_a^t = \mathcal{F}_{a_{\text{ip}}}^t \cup \mathcal{F}_{a_{\text{op}}}^t, \quad \mathcal{F}_{a_{\text{ip}}}^t = \left\{ \mathbf{P} \in \mathcal{F}_a^t, \; v \in [-1, +1] \right\}, \; \mathcal{F}_{a_{\text{op}}}^t = \left\{ \mathbf{P} \in \mathcal{F}_a^t, \; v \notin [-1, +1] \right\} \quad (9)$$

The set $\mathcal{F}_{a_{\text{ip}}}^t$ is formed by the nodes for which the closest point projection is inside a crack surface element; the set $\mathcal{F}_{a_{\text{op}}}^t$ is formed by the nodes for which the closest point projection is outside any crack surface element, but is potentially belonging to a kink wedge in the direction of the crack front. Note that the kink wedges in the direction of the advance vectors, i.e. the points whose projection
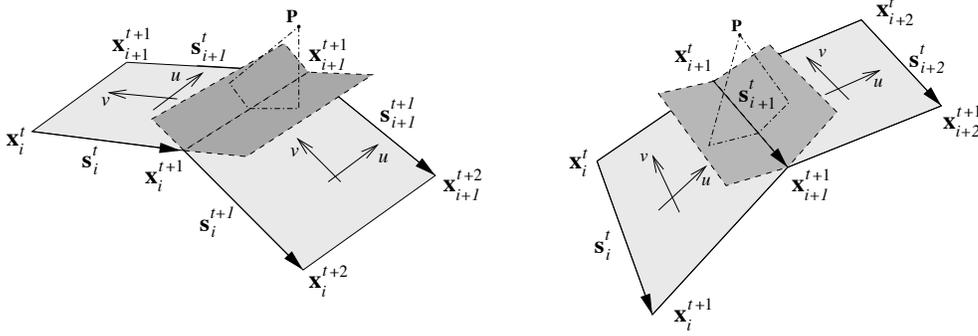
Figure 6: Projections of a point belonging to kink wedges onto the analytic continuations of two crack surface elements. On the left the kink wedge runs along a crack front, on the right the kink wedge runs along an advance vector.

on adjacent surface elements has the property $u \notin [-1, +1]$, are accounted for when looping on the crack front surface elements to determine the closest point projection. Here the necessity of distinguishing between the sets $\mathcal{F}^t_{a_{\mathrm{ip}}}$ and $\mathcal{F}^t_{a_{\mathrm{op}}}$ emanates from the fact that the kink wedges in the direction of the crack front are generated in between two subsequent time steps.

To this end the set $\mathcal{F}^t_{a_{\mathrm{op}}}$ is in turn split into the following two

$$\mathcal{F}^t_{a_{\mathrm{op}}} = \mathcal{F}^t_{a^+_{\mathrm{op}}} \cup \mathcal{F}^t_{a^-_{\mathrm{op}}}, \quad \mathcal{F}^t_{a^+_{\mathrm{op}}} = \left\{ \mathbf{P} \in \mathcal{F}^t_a,\, v > 1 \right\}, \mathcal{F}^t_{a^-_{\mathrm{op}}} = \left\{ \mathbf{P} \in \mathcal{F}^t_a,\, v < -1 \right\} \qquad (10)$$

The nodes belonging to $\mathcal{F}^t_{a^+_{\mathrm{op}}}$ have projection behind the crack surface advance, while the nodes belonging to $\mathcal{F}^t_{a^-_{\mathrm{op}}}$ have projection ahead the crack surface advance, see Fig. 6. Consequently the nodes belonging to the set $\mathcal{F}^{t-1}_{a^-_{\mathrm{op}}}$ at the time step $t-1$ and to the set $\mathcal{F}^t_{a^+_{\mathrm{op}}}$ at the time step t belong to a kink wedge. This allows for formulating the evolution law for the level set domain $\mathcal{F}$ as follows

$$\mathcal{F}^t = \mathcal{F}^{t-1} \cup \mathcal{Q}^t = \mathcal{F}^{t-1} \cup \mathcal{F}^t_{a_{\mathrm{ip}}} \cup \left(\mathcal{F}^{t-1}_{a^-_{\mathrm{op}}} \cap \mathcal{F}^t_{a^+_{\mathrm{op}}} \right) \qquad (11)$$

In (11) the set $\mathcal{Q}^t = \mathcal{F}^t_{a_{\mathrm{ip}}} \cup \left(\mathcal{F}^{t-1}_{a^-_{\mathrm{op}}} \cap \mathcal{F}^t_{a^+_{\mathrm{op}}} \right)$ determines the nodes to be included in the levelset domain at time t. For the nodes in $\mathcal{F}^t_{a_{\mathrm{ip}}}$, i.e. having closest point projection inside a crack surface element, the level set function is determined by solving (8) and then letting

$$f(\mathbf{P}_i, t) = \mathbf{P}'_i - \mathbf{P}_i = -\lambda \mathbf{n}; \quad H_f(\mathbf{P}_i, t) = \mathrm{sign}(\lambda) \quad \mathbf{P}_i \in \mathcal{F}^t_{a_{\mathrm{ip}}} \qquad (12)$$

On the other hand, for the nodes in $\mathcal{F}^{t-1}_{a^-_{\mathrm{op}}} \cap \mathcal{F}^t_{a^+_{\mathrm{op}}}$, i.e. belonging to a crack wedge and having closest point projection onto the crack front at the step $t-1$, the level set function is determined by computing the geometric closest point $\mathbf{P}'$ and then, being the solution to (8) known it is set

$$f(\mathbf{P}_i, t) = \mathbf{P}'_i - \mathbf{P}_i; \quad H_f(\mathbf{P}_i, t) = \mathrm{sign}(\lambda) \quad \mathbf{P}_i \in \mathcal{F}^{t-1}_{a^-_{\mathrm{op}}} \cap \mathcal{F}^t_{a^+_{\mathrm{op}}} \qquad (13)$$

7

Unlike (12), in (13) it is $\mathbf{P}' - \mathbf{P} \neq - \lambda\mathbf{n}$ as the projection is on the kink wedge and not on a surface element. In this case the solution to (8) is used for computing the sets $\mathcal{F}^{t-1}_{a_{\mathrm{op}}^{-}}$ and $\mathcal{F}^{t}_{a_{\mathrm{op}}^{+}}$ and for setting the sign of the distance.

Finally, with reference to (11), it is observed that in general it is $\mathcal{F}^{t-1} \cap \mathcal{Q}^t \neq \varnothing$. In fact, due to the change of the direction of the crack front, some points belonging to $\mathcal{F}^{t-1}$ may have a closer projection on the crack front at time t and the level set at the relevant points is redefined.

3.3 *Level set function g – Distance from the crack front*

The definition of the level set function g expressing the distance from the crack front is rather simpler than f. In fact, given the geometric crack front representation by line segments introduced in Sect. 3.1, we assume that the level set function g at a point $\mathbf{P}$ can be expressed through a vector $\mathbf{g}$ and a Boolean H_g assuming the values ± 1 and yielding the sign of the distance, i.e. telling if $\mathbf{P}$ lies ahead or behind the crack front, Fig. 4. The role of g in fracture modeling is that of evaluating the polar angle and distance used by branch function enrichments [13]. With reference to Fig. 4 and Fig. 2(b), $\mathbf{g}$ at $\mathbf{P}$ can be computed by closest point projection on the crack front, while H_g is evaluated by taking the opposite of the sign of the scalar product of $\mathbf{g}$ times the closest advance vector, i.e. $H_g = - \operatorname{sign}(\mathbf{g} \cdot \mathbf{s}^t)$.

The set of nodes where g is defined depends on the strategy used for the enrichment. In early XFEM works only the nodes of the elements containing the crack front (or tip in 2D) were enriched, while it was later recognized that to preserve the convergence rate [14, 15] and minimize blending effects [12, 16] an opportune number of layers of elements around the front is to be enriched. Once the branch functions enrichment domain is chosen the set of nodes where g is defined will be given by all the element nodes in the branch functions enrichment domain. The g domain and values will be recomputed at each step.

3.4 *Interpolation to non-nodal points*

For computational purposes the level set values are to be known at the elements Gauss points (for computing the stiffness matrices) and at the element nodes (for post-processing purposes). It is common practice in all approaches to compute and store level set values at element nodes and interpolate these values at the Gauss points by element shape functions interpolation. Other forms of interpolation may be used to get for example smooth crack representations, e.g. moving least squares or radial basis functions interpolations, but this topic is out of the scope of the present work. A similar approach, related to the representation of smooth contact surfaces can be found in [17].

4 NUMERICAL RESULTS

The proposed method for the representation of 3D crack surfaces does not depend on how the crack surface evolution is modeled but, given the crack front advance vectors, is purely geometric. Therefore, to test the method, it is not necessary to solve a particular mechanical problem, but it suffices to introduce a discretization mesh in a domain and a set of advance vectors for the crack front to observe the correct construction and evolution of the level set functions. The used domain is cubic and is illustrated in Fig. 7(a), discretized by 55177 tetrahedrons and 10231 nodes. Several crack propagation tests have been run to check the method in the most critical situations like crack kinks, crack front resampling and twisted cracks. Here only one result is presented for space restrictions. A flat crack propagates and curves back Fig. 7(b). The figure is taken at the end of the propagation process and illustrates the level sets f and g as well as the enriched tetrahedrons. The vectors $\mathbf{f}$ representing f are red if $H_f > 0$ and blue if $H_f < 0$, while the tetrahedrons to be enriched with the

Heaviside step function are plotted light yellow. The vectors **g** representing g are magenta if $H_g > 0$ and green if $H_g < 0$, while the tetrahedrons to be enriched with the crack front functions are plotted light cyan. The crack surface elements and advance vectors are plotted gray and black, respectively. Note that, compared to classical level set approaches, defining just the value of the distance, here the gradient of the distance functions is known as well. This information can be proficiently used to define splitting planes of the elements for quadrature purposes. In fact, being the enrichment functions discontinuous or singular, the finite elements need to be split into quadrature subcells, and the distance vector provided by the present approach provides the desired information.
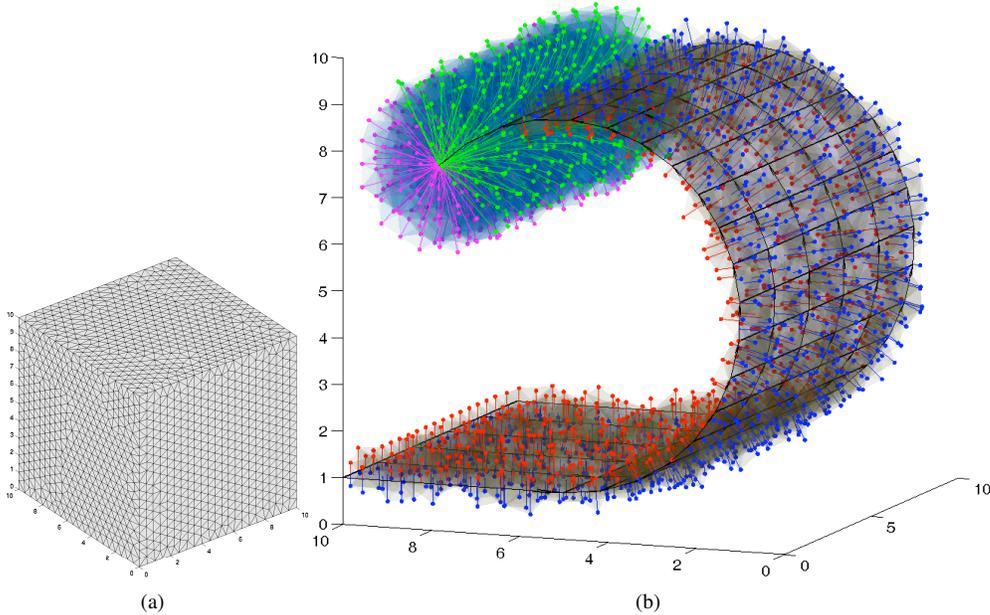

Figure 7: (a) The discretized domain used for numerical tests; (b) Results obtained for the curved crack example.

5 CONCLUSIONS

The proposed method extends to three dimensions the vector level set method presented in [11]. The method uses only geometric and vector tools to build the level set representation of a propagating crack surface and, compared to classical methods where a set of differential equations is to be solved, is therefore very simple to implement and numerically efficient. The method builds up automatically the lists of elements needing discontinuous or singular enrichment as well. The generated vector data can be proficiently used for the numerical integration of the enrichment functions at the element level.

References

[1] Moës, N., Dolbow, J. and Belytschko, T., "A finite element method for crack growth without remeshing," *Int. J. Numer. Meth. Eng.*, **46**, 131-150 (1999).

[2] Strouboulis, T., Babuška, I. and Copps, K., "The design and analysis of the Generalized Finite Element Method," *Comput. Method. Appl. M.*, **181**, 43-69 (2000).

[3] Osher, S. and Fedkiw, R.P. *Level Set Methods and Dynamic Implicit Surfaces*, Springer-Verlag New York (2003).

[4] Sethian, J.A., *Level set methods and fast marching methods*, Cambridge University Press, Cambridge (1999).

[5] Stolarska, M., Chopp, D.L., Moes, N. and Belytschko, T., "Modelling crack growth by level sets in the extended finite element method," *Int. J. Numer. Meth. Eng.*, **51**, 943-960 (2001).

[6] Sukumar, N., Chopp, D.L., Moës, N. and Belytschko, T., "Modeling holes and inclusions by level sets in the eXtended finite element method," *Comput. Method. Appl. M.*, **190**, 6183-6200 (2001).

[7] Sukumar, N., Chopp, D.L. and Moran, B., "Extended finite element method and fast marching method for three-dimensional fatigue crack propagation," *Eng. Fract. Mech.*, **70**, 29-48 (2003).

[8] Duflot, M., "A study of the representation of cracks with level sets," *Int. J. Numer. Meth. Eng.*, **70**, 1261-1302 (2007).

[9] Gravouil, A., Moës, N. and Belytschko, T., "Non-planar 3D crack growth by the extended finite element and level sets - Part II: Level set update," *Int. J. Numer. Meth. Eng.*, **53**, 2569-2586 (2002).

[10] Chessa, J., Smolinski, P. and Belytschko, T., "The extended finite element method (XFEM) for solidification problems," *Int. J. Numer. Meth. Eng.*, **53**, 1959-1977 (2002).

[11] Ventura, G., Budyn, E. and Belytschko, T., "Vector level sets for description of propagating cracks in finite elements," *Int. J. Numer. Meth. Eng.*, **58**, 1571-1592 (2003).

[12] Ventura, G., Gracie, R. and Belytschko, T., "Fast integration and weight function blending in the extended finite element method," *Int. J. Numer. Meth. Eng.*, **77**, 1-29 (2009).

[13] Belytschko, T., Moës, N., Usui, S. and Parimi, C., "Arbitrary discontinuities in finite elements," *Int. J. Numer. Meth. Eng.*, **50**, 993-1013 (2001).

[14] Ventura G., Moran B. and Belytschko T., "Dislocations by partition of unity," *Int. J. Numer. Meth. Eng.*, **62**, 1463-1487 (2005).

[15] Laborde, P., Pommier, J., Renard, Y. and Salaun, M., "High-order extended finite element method for cracked domains," *Int. J. Numer. Meth. Eng.*, **64**, 354-381 (2005).

[16] Fries T.-P., "A corrected XFEM approximation without problems in blending elements," *Int. J. Numer. Meth. Eng.*, **75**, 503-532 (2008).

[17] Belytschko, T., Daniel W.J.T. and Ventura G., "A monolithic smoothing-gap algorithm for contact-impact based on the signed distance function," *Int. J. Numer. Meth. Eng.*, **55**, 101-125 (2002).